Available online at www.sciencedirect.com
ScienceDirect
Journal of Power Sources 166 (2007) 310–316
JOURNAL OF POWER SOURCES
www.elsevier.com/locate/jpowsour

High activity PtPd-WC/C electrocatalyst for hydrogen evolution reaction

Mei Wu [a,b], Pei Kang Shen [a,*], Zidong Wei [b], Shuqin Song [a], Ming Nie [a,b]

[a] *State Key Laboratory of Optoelectronic Materials and Technologies, School of Physics and Engineering, Sun Yat-Sen University, Guangzhou 510275, PR China*
[b] *School of Chemical Engineering, Chongqing University, Chongqing 400044, PR China*

Received 7 December 2006; received in revised form 22 December 2006; accepted 22 December 2006
Available online 2 February 2007

Abstract

Pd modified Pt over a novel support of tungsten carbide nanocrystals (the catalyst denotes as PtPd-WC/C) have been prepared by using an intermittent microwave heating (IMH) method. The as-prepared electrocatalysts are characterized by using the techniques of XRD, SEM, TEM, linear sweeping voltammetry and tested for the hydrogen evolution reaction (HER) in the acidic media. It shows a better performance for the HER on PtPd-WC/C electrocatalyst than that on Pt-WC/C electrocatalyst. In addition, these effects on the catalytic activity by changing environmental temperature and electrolyte concentration were taken into account. Kinetic study shows that the HER on the PtPd-WC/C electrocatalyst gives higher exchange current density in H_2SO_4 solution with high concentration, leading to a lower overpotential and facile kinetics. XRD, SEM and TEM images of PtPd-WC/C show the crystalline features of Pt, Pd and tungsten carbides and indicated the coexistence of these components.

Keywords: Hydrogen evolution reaction (HER); PtPd-WC/C electrocatalyst; Tungsten carbide (WC); Fuel cell

1. Introduction

In recent years, hydrogen, in combination with fuel cells, has been proposed as a major energy source. Worldwide interest in moving toward a hydrogen economy has its basis on the prospect of meeting energy needs at less environmental damage, with greater efficiency and acceptable cost compared to the conventional fossil fuels [1]. The majority of hydrogen energy source is chemically bound to water and some is bound to liquid or gaseous hydrocarbons [2]. The chemical energy per mass of hydrogen is three times larger than that of the other chemical fuels. Until all technical problems related to storage and transportation of hydrogen is resolved, its generation is expected to be accomplished on-site by the reformation of various gaseous or liquid feed stocks. Biomass-derived materials, or bio-fuels, are viable alternatives for this purpose since they offer high-energy density and ease of handling, so that they can be used for on-demand production of hydrogen for automotive and distributed power generation. An important advantage of bio-fuels for hydrogen production is that their use is neutral or nearly without CO_2 emissions. It means that hydrogen will be central to our energy economy.

The growing demand for clean and efficient energy systems is the driving force in the development of hydrogen production technology, particularly, for power generation in fuel cells. Successful development of low cost, efficient fuel processing systems will be critical to the commercialization of this technology as Verykios's team have shown in their work [3–5]. Steam reforming is one of the main ways to produce hydrogen. Ni dispersed on La_2O_3 offers a catalyst for steam reforming of ethanol which is not only active and selective toward hydrogen production but also stable with time in steam, even under conditions which favor carbon formation and deposition. In addition, Raney Ni, Ni–Mo [6–8], Ni–S alloy and Ni–S–Zr alloy [9,10] have also been widely studied. Besides, noble metals such as Pt, Pd, Ru, etc. were also used in this field [11–13]. Although Pt and Pd have a high catalytic activity for hydrogen evolution reaction (HER), and Pd has a good capacity for hydrogen storage, their limited reserves in the earth restricts their wide application in industry [14,15]. Many scientists make large effort to find the other novel materials for HER to replace or reduce the use of noble metals [16–22].

* Corresponding author. Tel.: +86 20 84036736; fax: +86 20 84113369.
E-mail address: stsspk@mail.sysu.edu.cn (P.K. Shen).

0378-7753/$ – see front matter © 2007 Elsevier B.V. All rights reserved.
doi:10.1016/j.jpowsour.2006.12.108

Since Bohm found that tungsten carbide possessed promising catalytic activity in sulfuric acid solutions in 1968 [23], an increasing interest has been directed to the use of tungsten carbides in catalysis [24–31]. Tungsten carbide can also be used as the electrocatalyst for hydrogen evolution reaction [25,32]. However, tungsten carbide alone cannot be directly used for HER due to the fact that HER has a high overpotential on it, consequently leading to the high electricity consumption, which makes the process economically unattractive, counteracting the associated technical and environmental advantages. Our previous results showed that tungsten carbide promoted Pt/C electrocatalysts exhibited a promising performance for hydrogen evolution.

The aim of the present work is to develop novel electrocatalysts based on tungsten carbides for hydrogen evolution in acid solution. Pd has already been widely used as the catalyst for HER in alkaline media [18–20,33–38], but in acid media there are few reports. In this paper, Pd was adulterated into Pt-WC/C by microwave heating method. The morphology, crystal structure and the composition of the electrocatalysts was characterized by X-ray diffraction (XRD), transmission electron microscopy (TEM), scanning electron microscopy (SEM) in conjunction with energy dispersive X-ray spectroscopy (EDX). The catalytic activity of the as-prepared electrocatalysts was evaluated by the techniques of cyclic voltammetry and linear potential sweep. The factors (the catalysts' composition, temperature, electrolyte concentration and potential scan rate) influencing the HER activity were also investigated.

2. Experimental

2.1. Preparation

Chemicals were of analytical grade purity and used as received. All the solutions were freshly prepared with distilled-deionized water. Tungsten powder (1.0 g) was added to 25.0 ml of aqueous solution containing 10.0 ml of 30% (v/v) H_2O_2, 5.0 ml 2-propanol and 10.0 ml water. The solution was left for the complete dissolution of tungsten powder before 1.0 g Vulcan XC-72 carbon powder (Cabot Corp., USA) was added. The mixture was then treated in an ultrasonic bath to form uniformly dispersed ink. After that, the well-mixed ink was dried in a microwave oven with an intermittent microwave heating (IMH) procedure as reported previously [39]. Finally, the dried ink was further treated by the continuous microwave heating till the formation of the tungsten carbide in argon atmosphere.

The corresponding salt of Pd was reduced by $NaBH_4$ on the mixture of as-prepared tungsten carbide and 50 wt% Pt/C (Johnson Matthey Corp.). In order to make the catalyst well distributed, the above mixture was stirred in an ultrasonic bath with 2-propanol (drops) for 20 min to obtain composite electrocatalysts.

The graphite rod with a diameter of 6.0 mm was used as electrode substrate and the top surface of the rod was pre-cleaned. The mixture was treated ultrasonically for 20 min for the uniform dispersion in pure 2-propanol. A fixed quantity of mixture was then dropped onto the top surface of the graphite rod to prepare electrodes with different electrocatalyst loadings. Finally, a drop of 0.5 wt% Nafion suspension (DuPont, USA) was covered on the top to prevent the damage of the electrocatalyst layer. Table 1 summarizes the samples with different percentages of the components.

Table 1
Summary of the different electrocatalyst compositions

Reagent no.	Pt/C (mg)	$PdCl_2$ (mg)[a]	WC (mg)	Quantity of catalyst on per cm^2
Pd-WC/C	–	1.003	1.0	100 μgPd–100 μgWC
Pt/C	2.0	–	–	200 μgPt
Pt-WC/C	2.0	–	1.0	100 μgPt–100 μgWC
PtPd/C	2.0	1.003	–	100 μgPt–100 μgPd
PtPd-WC/C	2.0	1.003	2.0	50 μgPt–50 μgPd–100 μgWC

[a] The concentration of $PdCl_2$ is 5.9 mg ml^{-1}.

2.2. Characterization

The particle size and distribution of the samples were analyzed on a JOEP JEM-2010 high-resolution transmission electron microscopy (JEOL Ltd.) operating at 200 kV. X-ray diffraction was employed to obtain the information of the surface and bulk structure of the electrocatalysts and was carried out on a D/Max-IIIA diffratometer (Rigaku Co., Japan) employing Cu Kα (λ = 0.15418 nm) as the radiation source. The morphology and size of the electrocatalysts were characterized by scanning electron microscopy (LEO 1530VP, Germany) in conjunction with energy dispersive X-ray spectroscopy (EDX). Electrochemical measurements were performed on an IM6e Electrochemical workstation (Zahner-Electrik, Germany). A standard three-electrode electrolytic cell was used. The graphite rods coated with different electrocatalysts shown in Table 1 were adopted as the working electrode. A platinum foil and a saturated calomel electrode (SCE) were used as counter electrode and reference electrode, respectively. All potentials shown in these figures are against the standard hydrogen electrode (SHE).

3. Results and discussion

3.1. The effect of electrocatalyst composition on HER

The corresponding X-ray diffraction grams of the as-prepared WC and PtPd-WC/C are shown in Fig. 1a and b, respectively. The diffraction peaks at 31.52°, 35.66°, 36.98° and 48.32° with the *d* values of 2.8359, 2.5156, 2.4288 and 1.8819 correspond to (0 0 1), (1 0 0), (4 0 0) and (1 0 1) facets of WC. While the 2θ of 38.04°, 39.52°, 40.28° and 52.26° with the *d* values of 2.3635, 2.2783, 2.2371 and 1.7490 correspond to (2 0 0), (1 2 1), (1 0 2) and (2 2 1) facets of W_2C. In addition, the broad diffraction peak around 34° shows the overlapping of the peaks correspond to (0 2 1), (0 0 2) and (2 0 0) facets of W_2C. The results show that the tungsten carbides prepared by the present method exist as a mixture of WC and W_2C.

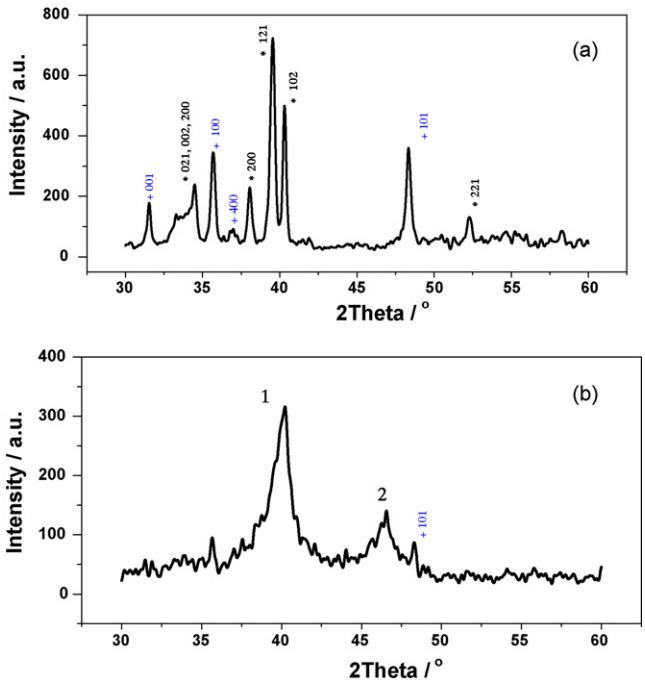

Fig. 1. XRD patterns of (a) WC and (b) PtPd-WC/C. *, W_2C; +, WC.

The diffraction peaks in Fig. 1b are broadening by the overlapping of these peaks with the closing d values. The peak marked 1 is identified as the overlapping of the (1 2 1) and (1 0 2) peaks of W_2C, (1 1 1) peak of Pt ($d = 2.265$) and (1 1 1) peak of Pd ($d = 2.246$). The peak 2 is the (2 0 0) peak both for Pt ($d = 1.962$) and Pd ($d = 1.945$). By comparing the standard d values, it is clear that the XRD pattern of PtPd-WC/C is a combined crystalline feature of Pt, Pd and tungsten carbides, indicating the coexistence of these components.

Fig. 2 shows the SEM micrographs of the PtPd-WC/C powder. The aggregation of the particles observed in the Fig. 2a is due to the active nature of the nano-scaled particles. However, it was demonstrated that the aggregated particles could be re-separated in an appropriate media. The enlarged micrograph (Fig. 2b) shows that the particles are in nanometer size and uniformly dispersed with a narrow size distribution.

Fig. 3 shows the typical transmission electron microscopic (TEM) images of Pt-WC/C and PtPd-WC/C, respectively. It can be clearly seen from Fig. 3 that both Pt-WC/C and PtPd-WC/C prepared by the IMH method are nano-sized and uniformly distributed. The average particle size is 2.0 ± 1.0 nm. Moreover, the EDX analysis (insets in Fig. 3a and b) on these small black dots demonstrates the coexistence of Pt, Pd and WC.

The linear potential sweep curves for HER over different electrocatalysts are illustrated in Fig. 4a. The total loadings of

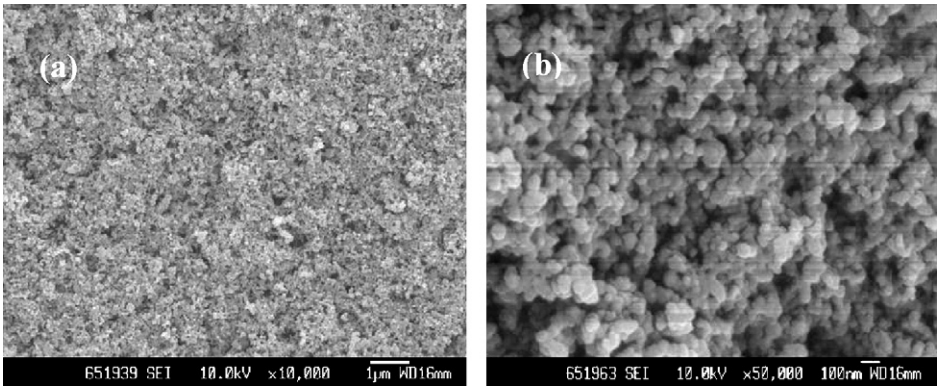

Fig. 2. SEM micrographs of PtPd-WC/C with the bar of (a) 1 μm and (b) 100 nm.

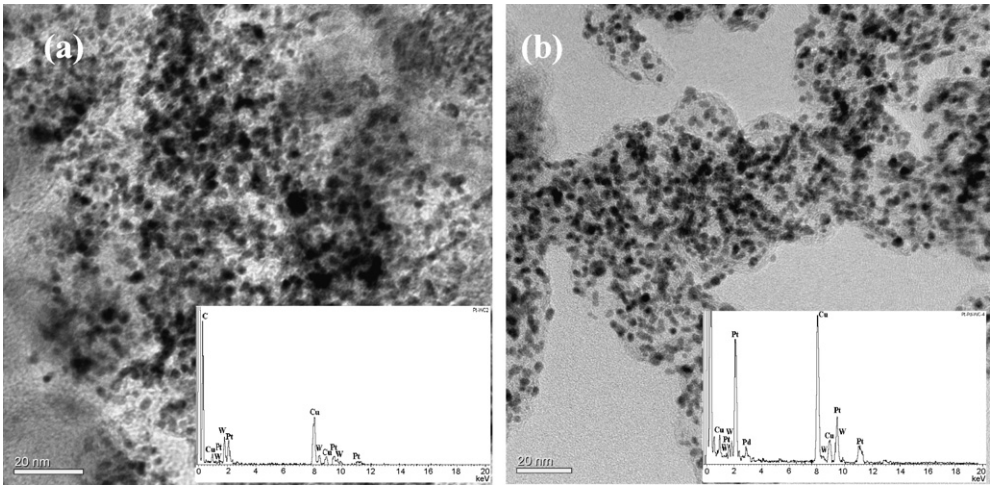

Fig. 3. TEM images of (a) Pt-WC/C, (b) PtPd-WC/C. Insets in (a) and (b) are the EDX patterns on these small black dots.

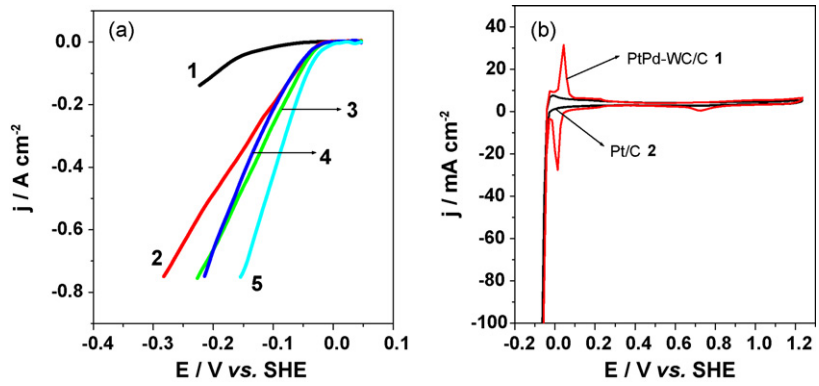

Fig. 4. (a) Linear potential sweep curves of the HER on different electrocatalysts in 0.5 mol dm^{-3} H_2SO_4 solution at 30 °C and (b) cyclic voltammograms at higher potential limits at 50 mV s^{-1} in the same solution. Scan rate: 5 mV s^{-1}. (a) 1, 100 μgPd/100 μgWC/C; 2, 200 μgPt/C; 3, 100 μgPt + 100 μgWC/C; 4, 100 μgPt + 100 μgPd/C; 5, 50 μgPt + 50 μgPd + 100 μgWC/C. (b) 1, 200 μgPt/C; 2, 50 μgPt + 50 μgPd + 100 μgWC/C.

the electrocatalyst were 200 μg for each electrode. The curve 1 obtained on a 100 μgPd/100 μgWC/C electrode showed a higher overpotential more than 100 mV compared to that on a 200 μgPt/C electrode (Fig. 4a-2). It was reported that HER on Pd had a higher overpotential in alkaline solution [4]. It means that Pd-WC/C alone as electrocatalyst is lack of the significance for HER. The performance of 100 μgPt/100 μgWC/C and 100 μgPt/100 μgPd/C electrodes is similar to 200 μgPt/C electrode at lower currenties, however, the increase in the overpotential with the increase in the current density is lower, showing a better performance. However, it can be clearly seen from Fig. 4a-5 that the addition of Pd nanocrystals into Pt-WC/C can significantly improve the activity for HER. PtPd-WC/C exhibits even better performance for HER than Pt-WC/C at higher Pt loadings from both the onset potential and current density point of views. It is clear that the slope of the current density against the overpotential was sharper for PtPd-WC/C than that for Pt-WC/C, indicating an increased kinetics. The effect of the Pd loading on the HER activity was also tested by changing the weight ratio of Pt to Pd. By comparing the HER performance of different electrodes in Fig. 4, when part of the Pt was replaced by Pd with the same weight of Pt, the current density can be significantly increased. It can be found that the electrode containing 50 μgPt, 50 μgPd, and 100 μgWC/C on each square centimeter possesses the best catalytic activity for HER.

Those CV curves of Pt/C and PtPd-WC/C in Fig. 4b are recorded in background solution. It shows that hydrogen adsorptive and desorptive peaks on PtPd-WC/C electrocatalyst is very sharp. Because of the hydrogen gas storage ability of Pd, there is much hydrogen centralizing in the PtPd-WC/C catalyst, and then the rich hydrogen in Pd sites was oxidized at the potential of 0 V. This is the reason that the oxidation peak appears sharply. It is also possible that the bigger hydrogen adsorptive/desorptive peaks corresponding to larger special area testified that some Pd adulterated in Pt-WC/C could increase the special area.

By comparing the kinetics of the hydrogen evolution/oxidation reactions (HER/HOR) on Pt (1 1 1) with Pt (1 1 1)-Pd, Marković et al. [40] tried to understand how the divergences in binding of the reaction intermediates to the Pt (1 1 1)–Pd surface, which these authors inferred from surface X-ray scattering (SXS) measurements, is related to the kinetics of the HER/HOR. The mechanism for the HOR on platinum-group metals in acid electrolytes is usually assumed to proceed by an initial adsorption of molecular hydrogen, which involves either slow dissociation of H_2 molecules into the atoms, Eq. (1), or dissociation into the ion and atom, Eq. (2), followed by a fast charge-transfer step, Eq. (3):

$$H_2 \xrightarrow{\text{rds}} H_{opd} + H_{opd} \quad (1)$$

$$H_2 \xrightarrow{\text{rds}} H^+ + H_{opd} + e^- \quad (2)$$

$$H_{opd} \leftrightarrow H^+ + e^- \quad (3)$$

"H_{opd}" denotes the weak absorption of hydrogen into the bulk lattice of Pd.

The above reactions can be usually referred to as the Tafel–Volmer – (steps 1 and 3) or Heyrovsky–Volmer – (steps 2 and 3). In Marković's recent analysis for the hydrogen reaction on Pt(1 1 1), they have assumed that, close to the hydrogen reversible potential, the kinetic parameters (such as the exchange current density, the Tafel slope and the activation energies) are the same for the HOR and HER. Consequently, at low overpotentials the mechanism for the HER would be the same as that for the HOR.

As palladium absorbs hydrogen, there exists another reaction. That is the adsorbed hydrogen atom penetrates through the Pd surface layer and moves into an internal bulk site. Zhang and co-workers call it the penetration reaction [41]:

$$Pd_sH_s + Pd_b \leftrightarrow Pd_s + Pd_bH_b$$

where subscripts s and b represent the surface and bulk states, respectively.

3.2. The effect of temperature on HER

On the basis of the thermodynamics of the Pd|H electrode, which includes various steps in the HER, diffusion and self-stress of H in Pd, Zhang et al. [42] have discussed the temperature effect on various aspects of the hydrogen absorption. Their

results indicated that the loading ratio of H to Pd decreases with increasing temperature for both galvanostatic and potentiostatic charging conditions, and its amplitude depends on the charging pattern, the chemical and electrochemical parameters of the Pd|H electrode. Moreover, they have found that the increase in temperature accelerates hydrogen absorption into palladium for both galvanostatic and potentiostatic charging conditions. The self-stress of H in Pd decreases with increasing temperature for galvanostatic charging, but it changes slightly for potentiostatic charging. Finally, their theory fits the available experimental results.

In our present work, we also investigated the effect of temperature on HER and the results are illustrated in Fig. 5. Fig. 5a gives *j–T* curves of the PtPd-WC/C electrode at the overpotential of −50 mV in Fig. 5b, in which the linear sweep voltammogram (LSV) was recorded in 0.5 mol dm^{-3} H_2SO_4 solution at the scan rate of 5 mV s^{-1} from 30 to 70 °C. Fig. 5a shows the influence of electrolytic temperature on the performance of PtPd-WC/C electrode. The current densities change with the different electrolytic temperature. Table 2 compares the current densities at a typical potential of −50 mV at different temperatures. Obviously, the suitable environmental temperature is at around 40 °C for HER on the PdPt-WC/C electrocatalysts.

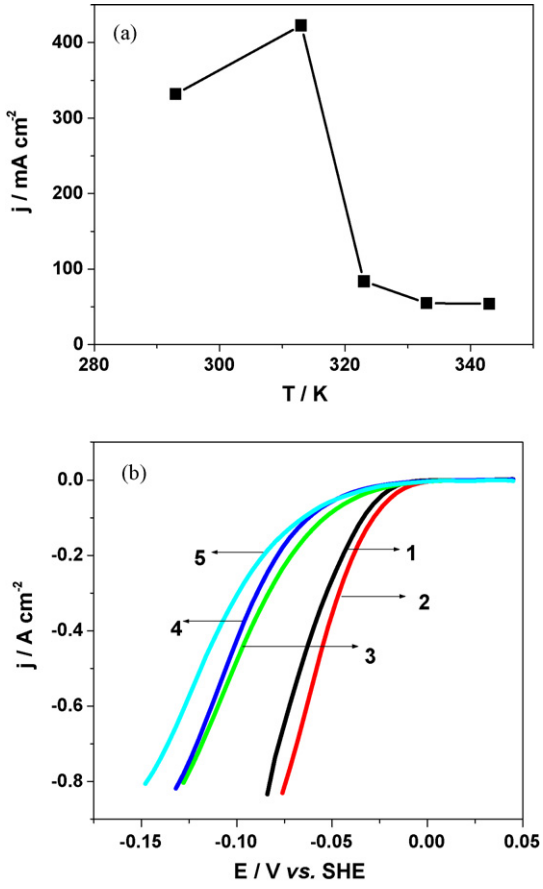

Fig. 5. Influence of the electrolytic cell temperature on the HER: (a) current density vs. *T* at the potential of −50 mV and (b) steady-state polarization curves of PtPd-WC/C electrode at different temperatures for HER in 0.5 mol dm^{-3} H_2SO_4 solution. Scan rate: 5 mV s^{-1}. 1, 303 K; 2, 313 K; 3, 323 K; 4, 333 K; 5, 343 K.

Table 2
Comparison of the performance for the HER on PtPd-WC/C at different temperatures in 0.5 mol dm^{-3} H_2SO_4 solution

T (K)	*j* (mA cm^{-2})
303	332
313	423
323	84
333	55
343	54

3.3. The effect of the electrolyte concentration on HER

In order to estimate quantitatively the electrochemical activity for HER in the acid electrolytes, Tafel plots of the electrodes were obtained in H_2SO_4 solution with different concentrations at 303 K. Shown in Fig. 6 is the influence of electrolyte concentration on the performance of PtPd-WC/C electrode for HER. It can be distinguished that the electrolyte concentration has an obvious effect on the polarization overpotential. The overpotential decreases with the increase in the acid concentrations from 0.1 to 2.0 mol dm^{-3} H_2SO_4. Compared to the onset potential of HER in the case of 0.1 mol dm^{-3} H_2SO_4 solution, the corresponding value is shifted positively more than 20 mV in 2.0 mol dm^{-3} H_2SO_4. The more positive onset potential and higher current density for HER at higher H_2SO_4 concentrations result from the obvious reason.

Fig. 6b shows the Tafel plots of PtPd-WC/C electrocatalysts in different concentrations of H_2SO_4 solution. It is well known that the intercept and slope of the Tafel plots can be obtained by the Tafel extrapolation technique, and then the exchange current density of HER, j°, can be calculated by the intercept and slope of the Tafel plots. The corresponding kinetic parameters are calculated from the curves in Fig. 6b and listed in Table 3.

It is apparent that the influence of the sulfuric acid concentration on HER activity on PtPd-WC/C electrode is significant. With increasing electrolyte concentration, the onset potential (η) increase gradually, which means that the electrocatalytic property of PtPd-WC/C electrocatalyst was improved. The positive onset potential shown in Table 3 for curve 3 in Fig. 4b is due to the pH effect which can be calibrated by using Nernest equation. The *a* and *b* in Table 3 are the intercept and slope values according to the Tafel plot:$\eta = a + b \lg j^\circ$, $a = (2.3RT/\alpha F) \lg j^\circ$, $b = -2.3RT/\alpha F$ [43]. The exchange current density (j°) shown in column 5 is remarkably increased at higher acid concentrations from 1.214×10^{-4} A cm^{-2} for 0.1 mol dm^{-3} H_2SO_4 to 18.776×10^{-4} A cm^{-2} for 2.0 mol dm^{-3} H_2SO_4. The results indicated that the concentration polarization on PtPd-WC/C electrocatalyst is critical. The improvement in the kinetics of the HER in H_2SO_4 solution at higher concentrations is the evidence that the increase in the H_2SO_4 concentration decreases the concentration polarization. These apparent results are significant, however, the kinetic processes are the same in nature. The j° values are very close after the concentration correction as shown in column 6 in Table 3.

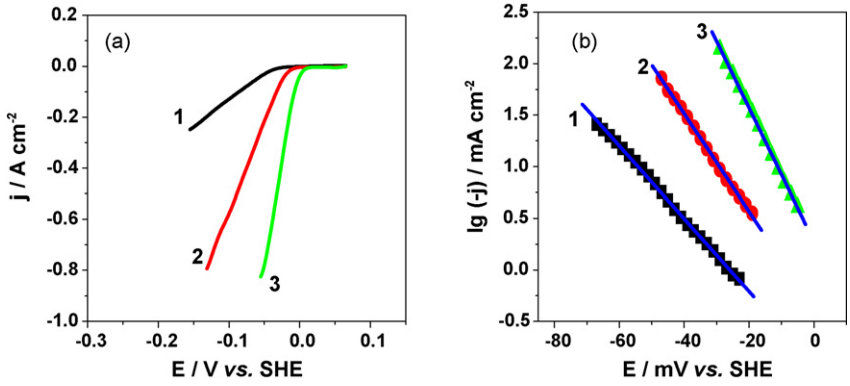

Fig. 6. The influence of electrolyte concentration on HER: (a) steady-state polarization curves and (b) Tafel plots of PtPd-WC/C electrode for HER in H_2SO_4 solutions of different concentrations. Scan rate: 5 mV s^{-1}. 1, 0.1 mol dm^{-3} H_2SO_4; 2, 0.5 mol dm^{-3} H_2SO_4; 3, 2.0 mol dm^{-3} H_2SO_4.

Table 3
Comparison of kinetic parameters for HER on PtPd-WC/C electrocatalysts in different concentrations of H_2SO_4 aqueous solutions

$C_{H_2SO_4}$ (mol dm^{-3})	Onset potential mV vs. SHE	Tafel slope, b ($\times 10^{-2}$ A m^{-2} V^{-1})	a ($\times 10^{-3}$ V)	$-j^\circ$ ($\times 10^{-4}$ A cm^{-2})	$-j^\circ$ ($\times 10^{-4}$ A cm^{-2}) (concentration corrected)
0.1	−30	−28.329	−25.946	1.214	8.10
0.5	−5	−21.097	−8.070	4.145	9.16
2.0	20	−15.432	4.222	18.776	10.65

4. Conclusions

The IMH method was successfully employed to prepare well-distributed and nanometer-sized PtPd-WC/C electrocatalysts and the as-prepared PtPd-WC/C was adopted as the electrocatalyst for hydrogen evolution reaction in acidic media for the first time. The voltammetric results indicated that the adulteration of Pd can significantly increase the activity of Pt-WC/C for HER, probably due to the specific function of Pd for hydrogen storage. It suggests that PtPd-WC/C has a potential application in the hydrogen production. The further investigation showed that the temperature obviously affects the HER activity with a desirable result at 313 K and a higher concentration of H_2SO_4 is favorable for the HER.

Acknowledgements

The authors gratefully acknowledge the support by the NNSF of China (20476108, 20476109), the NSF of Guangdong Province (04105500), the Guangzhou Science and Technology Key Project (2006Z3-C7031) and the Guangdong Science and Technology Key Project (2005A11004001).

References

[1] M. Manzoli, A. Chiorino, F. Boccuzzi, Appl. Catal. B 57 (2004) 201.
[2] H. Henry, H. Wu, J.G. Chen, J. Phys. Chem. B 107 (2003) 2029.
[3] A.N. Fatsikostas, D.I. Kondarides, X.E. Verykios, Catal. Today 75 (2002) 145.
[4] V. Klouz, V. Fierro, P. Denton, H. Katz, J. Lisse, S. Bouvot-Mauduit, C. Irodatos, J. Power Sources 105 (2002) 26.
[5] V. Galvita, G. Semin, V. Belyaev, V. Semikolenov, P. Tsiakaras, V. Sobyanin, Appl. Catal. A 220 (2001) 123.
[6] Q. Han, K.R. Liu, J.S. Chen, X.J. Wei, Int. J. Hydrogen Energy 28 (2003) 120.
[7] I. Paseka, Electrochim. Acta 47 (2001) 921.
[8] S. Mandal, D. Roy, R.V. Chaudhari, M. Sastry, Chem. Mater. 16 (2004) 3714.
[9] M.D. Curtis, M.D. McClain, Chem. Mater. 8 (1996) 936.
[10] J.P. Carpenter, C.M. Lukehart, S.B. Milne, D.O. Henderson, R. Mu, S.R. Stock, Chem. Mater. 9 (1997) 3164.
[11] W.K. Hu, J.Y. Lee, Int. J. Hydrogen Energy 23 (1998) 253.
[12] M.J. Degiz, G. Filho, E.R. Gonzalez, S. Srlnivasan, Int. J. Hydrogen Energy 20 (1995) 423.
[13] S. Martinez, M. Metiko¡š-Hukovi, L.J. Valek, Mol. Catal. A-Chem. 245 (2006) 114.
[14] Z. Mme, H. Abdel, J. Pagetti, J. Talbot, Mater. Chem. 2 (1977) 83.
[15] K. Ashok, Vijh. Mater. Chem. 4 (1979) 51.
[16] O. Savadogo, K. Amuzgar, D.L. Piron, Int. J. Hydrogen Energy 15 (1990) 783.
[17] T.H. Yang, S. Pyum, J. Electroanal. Chem. 414 (1996) 127.
[18] M. Baldauf, D.M. Kolb, Electrochim. Acta 38 (1993) 2145.
[19] K. Ohkawa, K. Hashimoto, A. Fujishima, Y. Noguchi, S. Nakayama, J. E. Chem. 1–2 (1993) 445.
[20] D.L. Boxall, C.M. Lukehart, Chem. Mater. 13 (2001) 806.
[21] N. Tateishi, K. Yahikozawa, K. Nishimura, Y. Takasu, Electrochim. Acta 37 (1992) 2427.
[22] P.C. Searson, A.E. Metallurgica, Materialia 39 (1991) 2519.
[23] H. Bohm, Nature 227 (1970) 483.
[24] R.B. Levy, M. Boudart, Science 181 (1973) 547.
[25] G.H. Li, C.A. Ma, Y.F. Zheng, W.M. Zhang, Micropor. Mesopor. Mater. 85 (2005) 234.
[26] R. Ganesan, J.S. Lee, Angew. Chem. Int. Ed. 44 (2005) 6557.
[27] M. Metikoš-Huković, Z. Grubač, N. Radić, A. Tonejc, J. Mol. Catal. A-Chem. 249 (2006) 172.
[28] S. Shanmugam, D.S. Jacob, A. Gedanken, J. Phys. Chem. B109 (2005) 19056.
[29] P.K. Shen, Z.Q. Tian, Electrochim. Acta 49 (2004) 3107.
[30] H.H. Nersisyan, H.I. Won, C.W. Won, Mater. Lett. 59 (2005) 3950.
[31] J.D. Oxley, M.M. Mdleleni, K.S. Suslick, Catal. Today 88 (2004) 139.

[32] L. Schlapbach, A. Züttel, Nature 414 (2001) 353.
[33] K. Kunimatsu, H. Uchida, M. Osawa, M. Watanabe, J. Electroanal. Chem. 587 (2006) 299.
[34] H. Yoshitake, T. Kikkawa, G. Mutt, K.I. Ota, J. Electroanal. Chem. 396 (1995) 491.
[35] M.E. Martins, C.F. Zinola, G. Andreasen, R.C. Salvarezza, A.J. Arvia, J. Electroanal. Chem. 445 (1998) 135.
[36] L.I. Antropov, Theoretical Electrochemistry, 2nd ed., Mir Publishers, Moscow, 1967, p. 436.
[37] M.R.G. Chialvo, A.C. Chiatvo, J. Electroanal. Chem. 372 (1994) 209.
[38] S. Szpak, C.J. Gabricl, J.J. Smith, R.J.J. Nowak, Electroanal. Chem. 309 (1991) 273.
[39] H. Meng, P.K. Shen, Chem. Commun. (2005) 4408.
[40] N.M. Marković, C.A. Lucas, V. Climent, V. Stamenković, P.N. Ross, Surf. Sci. 465 (2000) 103.
[41] W.S. Zhang, X.W. Zhang, H.Q. Li, J. Electroanal. Chem. 434 (1997) 31.
[42] W.S. Zhang, Z.L. Zhang, X.W. Zhang, J. Electroanal. Chem. 481 (2000) 13.
[43] A.J. Bard, L.R. Faulkner, Electrochemical Methods and Fundamental and Applications, 2nd ed., John Wiley & Sons, Inc., 2003 (Chapter 3.3).